Supporting Information

"Mechanistic Studies on the N-Alkylation of Amines with Alcohols Catalysed by Iridium(I) Complexes with Functionalized N-Heterocyclic Carbene Ligands"

M. Victoria Jiménez, Javier Fernández-Tornos, Miguel González-Lainez, Beatriz Sánchez-Page, Francisco J. Modrego, Luis A. Oro and Jesús J. Pérez-Torrente**

Departamento de Química Inorgánica, Instituto de Síntesis Química y Catálisis Homogénea-ISQCH, Universidad de Zaragoza-CSIC, 50009-Zaragoza, Spain.

Experimental procedure for the isolation of N-alkylated amine products.

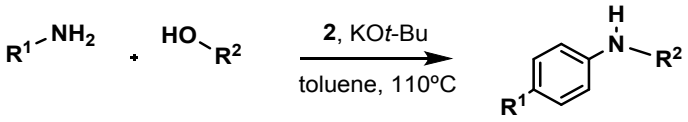

The catalytic N-alkylation reactions were carried out under an argon atmosphere in thick glass reaction tubes fitted with a greaseless high-vacuum stopcock. In a typical experiment, the reactor was charged with a solution of the amine (3.0 mmol) and the alcohol (3.0 mmol) in toluene (0.3 mL), internal standard (mesitylene, 70 μL, 0.5 mmol), base (KO*t*-Bu, 1.5 mmol) and the catalyst (0.03 mmol, 1 mol%). The resulting mixture was stirred at room temperature until complete solution of the catalyst and then placed in a thermostated oil bath at 110 ºC until completeness of the reaction. The reaction mixture was cooled to room temperature and all volatiles were removed under vacuum. Then water (5 mL) was added to the residue and extracted with diethyl ether (3x10 mL). The combined organic layers were dried over $MgSO_4$, filtered and the solvent removed under vacuum. The residue was dissolved with 3 ml hexane and then eluted through a silica gel column using hexane/diethyl ether (typically 5:1) as eluent.

***N*-benzylaniline**, R^1 = Ph, R^2 = CH_2Ph (Table 3, entry 1). Purification by column chromatography (hexano:diethyl ether, 5:1), 505 mg, 92%. ^1H NMR (300 MHz, $CDCl_3$, ppm): δ: 7.44-7.32 (m, 5H), 7.22 (t, *J* = 8.0 Hz, 2H), 6.76 (t, *J* = 7.3 Hz, 1H), 6.68 (d, *J* = 8.0 Hz, 2H), 4.38 (s, 2H), 4.06 (s_br, 1H). $^{13}C\{^1H\}$ NMR (300 MHz, $CDCl_3$, ppm): δ: 148.2, 139.5 (C), 129.3, 128.6, 127.5, 127.2, 117.6, 112.9 (CH), 48.4 (CH_2). The NMR data are consistent with those previously reported [T. Kawakami, T. Sugimoto, I. Shibata, A. Baba, H. Matsuda and N. Sonoda, *J. Org.Chem.*, **1995**, *60*, 2677-2682; H. Kato, I. Shibata, Y. Yasaka, S. Tsunoi, M. Yasudaa and A. Baba *Chem. Commun.*, **2006**, 4160-4168; B. Blank, M. Madalska, B. Blank, M. Madalska, R. Kempe, *Adv. Synth. Catal.* **2008**, *350*, 749–758].

***N*-hexylaniline** R^1 = Ph, R^2 = $(CH_2)_6$ (Table 3, entry 9): Purification by column chromatography (hexano:diethyl ether, 5:1), 516 mg, 97%. ^1H NMR (300 MHz, $CDCl_3$, ppm): δ: 7.21 (t, *J* = 7.5 Hz, 2H), 6.72 (t, *J* = 7.2 Hz, 1H), 6.64 (d, *J* = 8.3 Hz, 2H), 3.62 (s_br, 1H), 3.14, 1.65, 1.41, 1.37 (m, 10H), 0.94 (t, *J* = 6.6 Hz, 3H). $^{13}C\{^1H\}$ NMR (300 MHz, $CDCl_3$, ppm): δ: 148.6, (C), 129.2, 117.1, 112.7 (CH), 44.0, 31.7, 29.6, 26.9, 22.6 (CH_2), 14.0 (CH_3). The NMR data are consistent with those previously reported [M. Yus, J. Barluenga *J. Org. Chem*. **1982**, *47*,

156 0–1564; E. Byun, B. Hong, K. A. De Castro, M. Lim, H. Rhee *J. Org. Chem.* **2007**, *72*, 9815–9817].

***N*-phenethylaniline** R^1 = Ph, R^2 = $(CH_2)_2Ph$ (Table 3, entry 10): Purification by column chromatography (hexano:diethyl ether, 5:1), 497 mg, 84%. ^1H NMR (300 MHz, $CDCl_3$, ppm): δ: 7.40-7.21 (m, 7H), 6.76 (t, *J* = 6.7Hz, 1H), 6.67 (d, *J* = 8.1 Hz, 2H), 3.70 (s_br, 1H) 3.46, (t, *J* = 8.1 Hz, 2H), 2.96 (t, *J* = 8.1 Hz, 2H). $^{13}C\{^1H\}$ NMR (300 MHz, $CDCl_3$, ppm): δ: 148.0, 139.3 (C), 129.3, 128.8, 128.6, 126.4, 117.5, 113.0 (CH), 45.1, 35.6 (CH_2). The NMR data are consistent with those previously reported [M. Beller, O. R. Thiel, H. Trauthwein, C. G. Hartung, *Chem. Eur. J.* **2000**, *6*, 2513 –2522; A. S. Gajare, K. Toyota, M. Yoshifuji, F. Ozawa *J. Org. Chem.*, **2004**, 69, 6504–6506; K. Fujita, Y. Enoki, R. Yamaguchi, *Tetrahedron* **2008**, *64*, 1943–1954].

***N*-benzyl-4-methyl-aniline** R^1 = *p*-CH_3-C_6H_4, R^2 = CH_2Ph (Table 4, entry 2): Purification by column chromatography (hexano:diethyl ether, 5:1), 491 mg, 83%. ^1H NMR (300 MHz, $CDCl_3$, ppm): δ: 7.44-7.32 (m, 5H), 7.05 (d, *J* = 8.3 Hz, 2H), 6.69 (d, *J* = 8.3 Hz, 2H), 4.36 (s, 2H), 4.04 (s_br, 1H), 2.30 (s, 3H). $^{13}C\{^1H\}$ NMR (300 MHz, $CDCl_3$, ppm): δ: 145.8, 139.6 (C), 129.8, 128.6, 127.6, 127.2 (CH), 126.9 (C), 113.2 (CH), 48.8 (CH_2), 20.4 (CH_3). The NMR data are consistent with those previously reported [D. B. Bagal, R. A. Watile, M. V. Khedkar, K. P. Dhake, B. M. Bhanage, *Catal. Sci. Technol.*, **2012**, *2*, 354–358].

***N*-phenethyl-4-methyl-aniline** R^1 = *p*-CH_3-C_6H_4, R^2 = $(CH_2)_2Ph$ (Table 4, entry 7): Purification by column chromatography (hexano:diethyl ether, 5:1), 526 mg, 83%. ^1H NMR (300 MHz, $CDCl_3$, ppm): δ: 7.38-7.25 (m, 5H), 7.04 (d, *J* = 7.7 Hz, 2H), 6.59 (d, *J* = 7.7 Hz, 2H), 3.43 (d, *J* = 7.2 Hz, 4H), 2.95 (d, *J* = 7.2 Hz, 2H), 2.29 (s, 3H). $^{13}C\{^1H\}$ NMR (300 MHz, $CDCl_3$, ppm): δ: 145.8, 139.4 (C), 129.8, 128.8, 128.6 (CH), 126.7 (C), 126.4, 113.3 (CH), 45.5, 35.6 (CH_2), 20.4 (CH_3). The NMR data are consistent with those previously reported [X. Cui, Y. Zhang, F. Shi, Y. Deng, *Chem. Eur. J.* **2011**, *17*, 2587–2591; D. Jaspers, S. Doye, *Synlett* **2011**, 1444–1448].

Dibenzylamine R^1 = CH_2Ph, R^2 = CH_2Ph (Table 4, entry 12): Purification by column chromatography (hexano:diethyl ether, 1:1), 495 mg, 81%. ^1H NMR (300 MHz, $CDCl_3$, ppm): δ:

7.42-7.28 (m, 10H), 3.85 (s, 4H), 2.27 (s_br, 1H). $^{13}C\{^{1}H\}$ NMR (300 MHz, $CDCl_3$, ppm): δ: 139.9, 128.6, 128.5, 127.5 (CH), 52.2 (CH_2), 20.4 (CH_3). The NMR data are consistent with those previously reported [O. Y. Lee, K. -L. Law, D. Yang, *Org. Lett.,* **2009**, *11*, 3302–3305].

***N*-benzyl-*N*-phenethylamine** R^1 = CH_2Ph, R^2 = CH_2CH_2Ph (Table 4, entry 14): Purification by column chromatography (diethyl ether), 576 mg, 91%. ^{1}H NMR (300 MHz, $CDCl_3$, ppm): δ: 7.35-7.22 (m, 10H), 3.85 (s, 2H), 2.91 (m, 4H), 1.94 (s_br, 1H). $^{13}C\{^{1}H\}$ NMR (300 MHz, $CDCl_3$, ppm): δ: 139.9, 139.8, 129.4, 129.0, 128.7, 128.6, 128.4, 128.3, 128.1, 127.5, 126.9, 126.1 (CH), 53.7, 50.4, 36.2 (CH_2). The NMR data are consistent with those previously reported [S. Kuhl, R. Schneider, Y. Fort, *Organometallics* **2003,** *22,* 4184–4186; K. Fujita, Y. Enoki, R. Yamaguchi, *Tetrahedron* **2008**, *64*, 1943–1954; R. Kawahara, K. Fujita, R. Yamaguchi, Adv. Synth. & Catal., **2011**, *353*, 1161–1168].

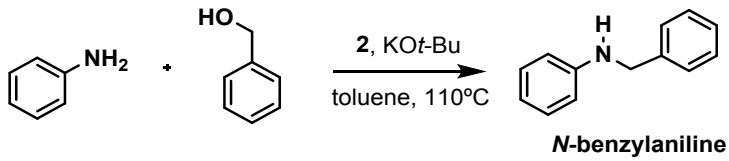

***N*-benzylaniline**

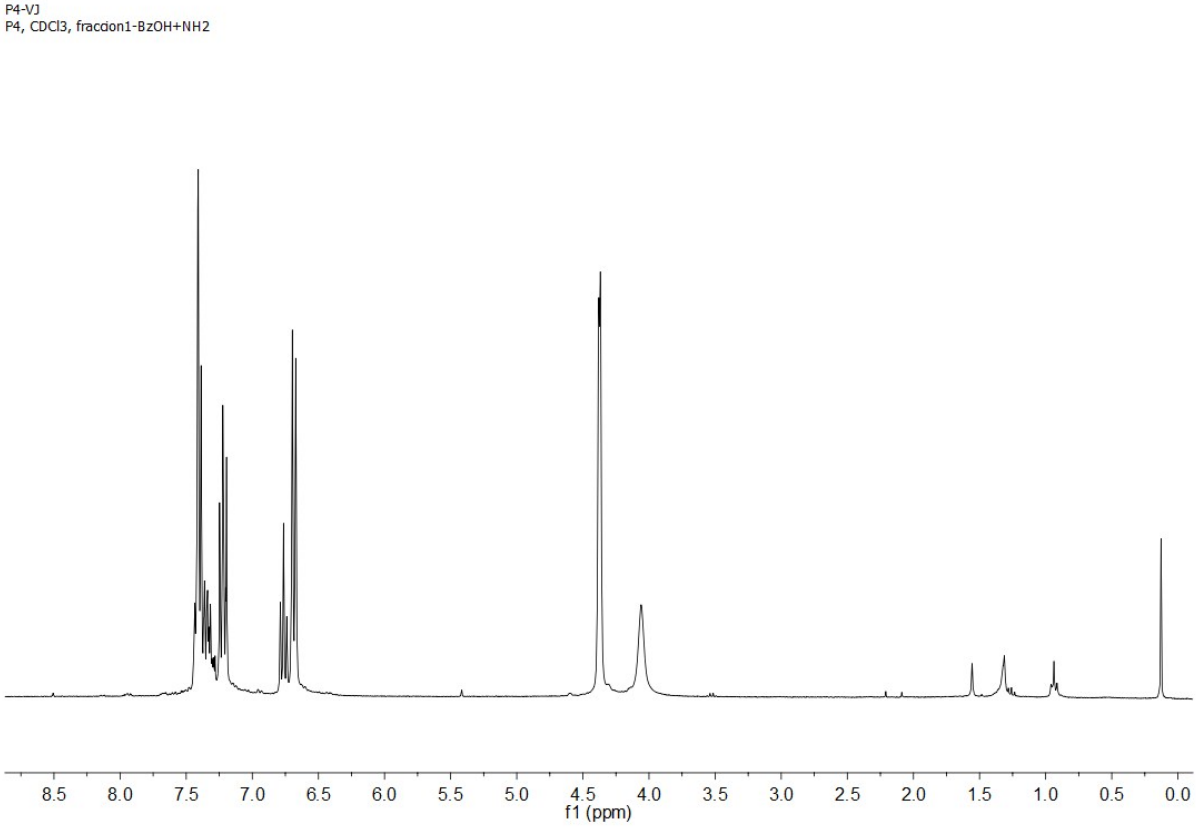

Figure S1. ^{1}H ($CDCl_3$, 298 K) NMR spectrum of *N*-benzylaniline.

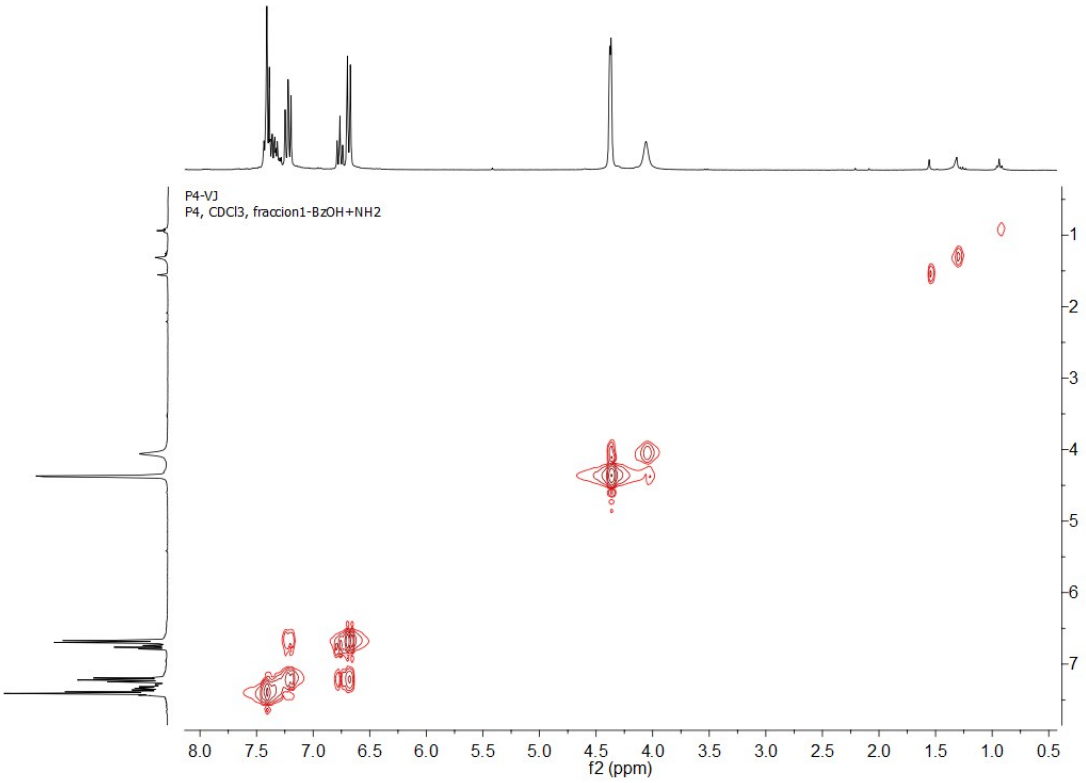

Figure S2. ^{1}H-^{1}H-cosy ($CDCl_3$, 298 K) NMR spectrum of *N*-benzylaniline.

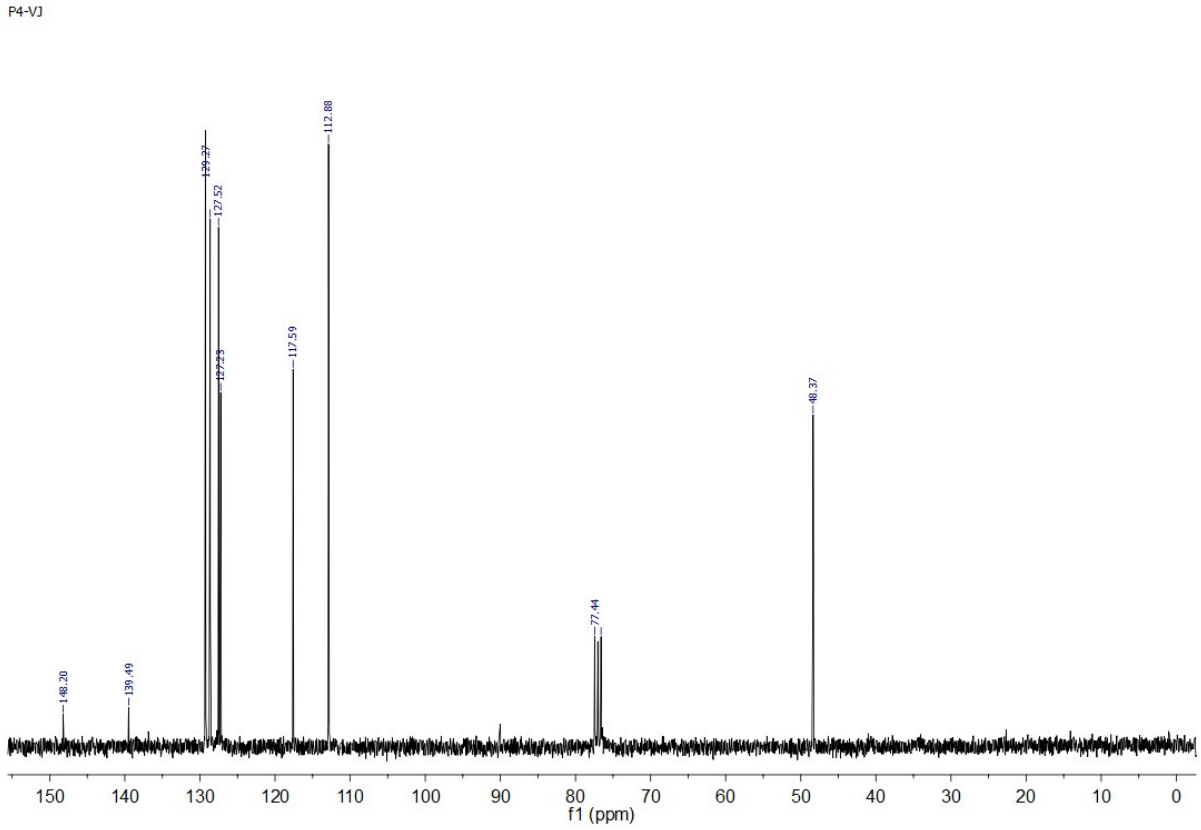

Figure S3. ^{13}C{^{1}H} ($CDCl_3$, 298 K) NMR spectrum of *N*-benzylaniline.

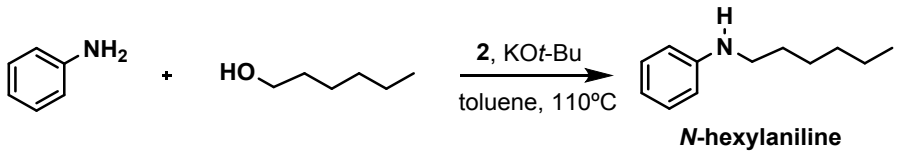

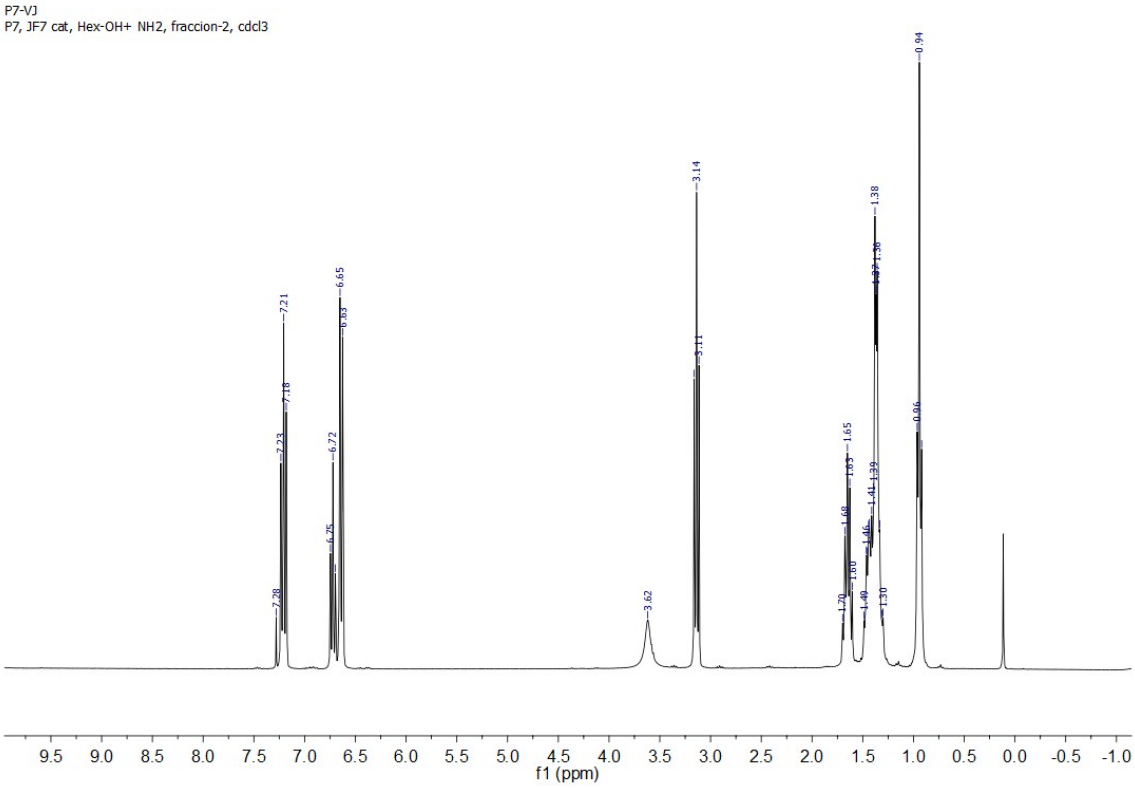

Figure S4. ^{1}H ($CDCl_3$, 298 K) NMR spectrum of *N*-hexylaniline.

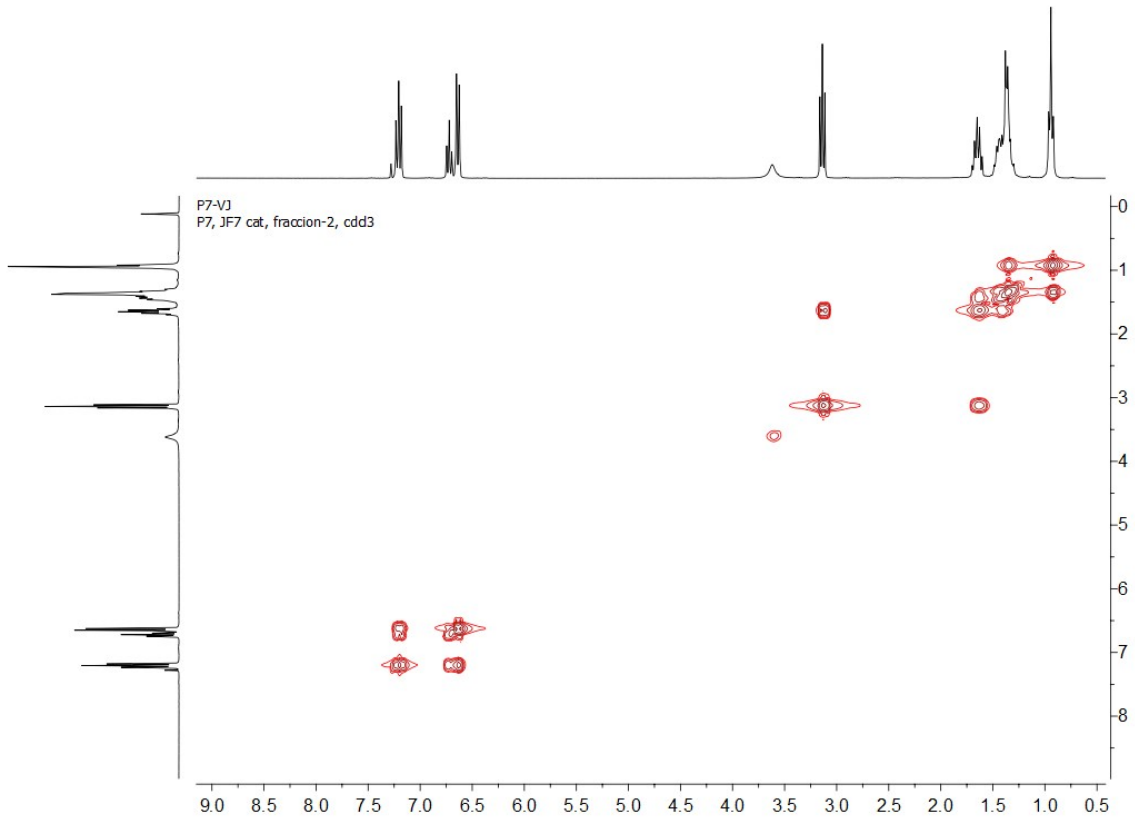

Figure S5. ^{1}H-^{1}H-cosy ($CDCl_3$, 298 K) NMR spectrum of *N*-hexylaniline.

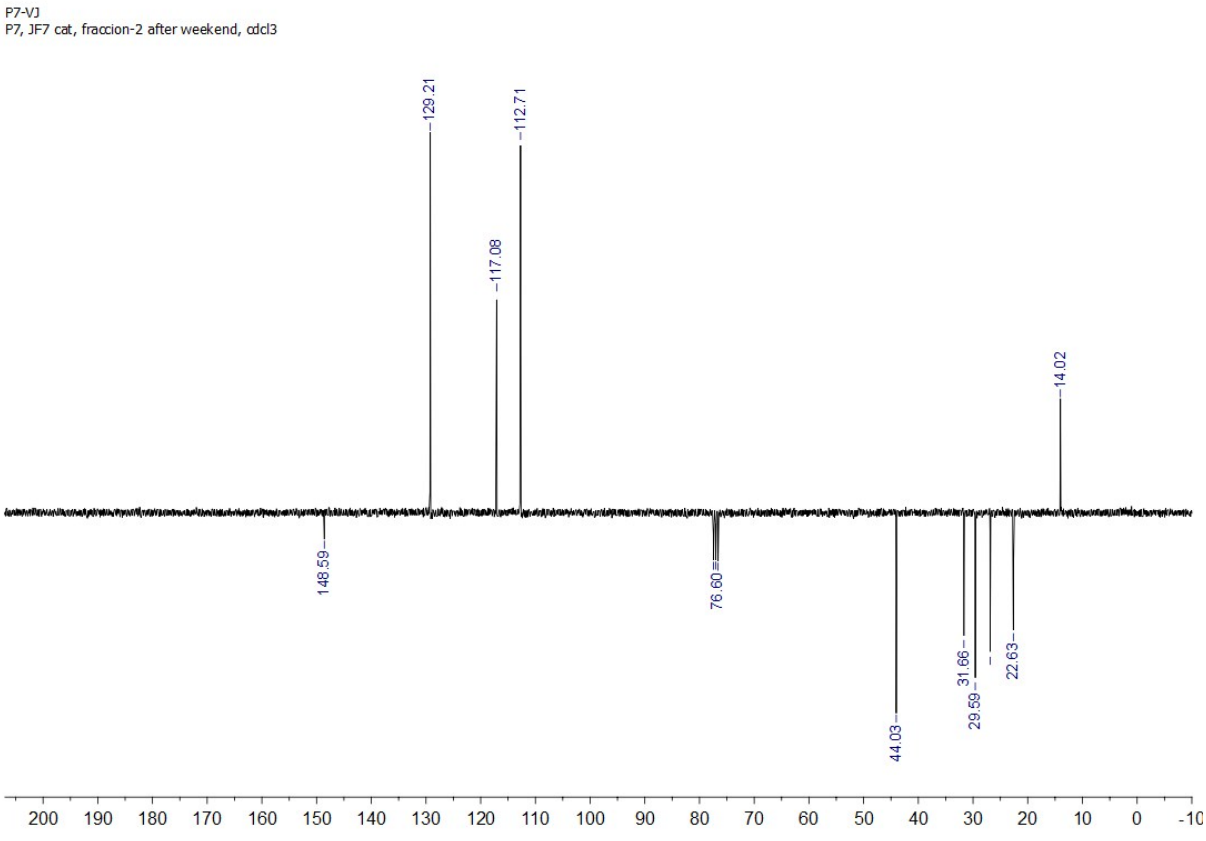

Figure S6. ^{13}C{^{1}H}-apt ($CDCl_3$, 298 K) NMR spectrum of *N*-hexylaniline.

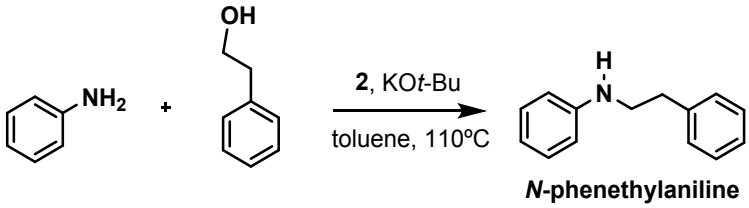

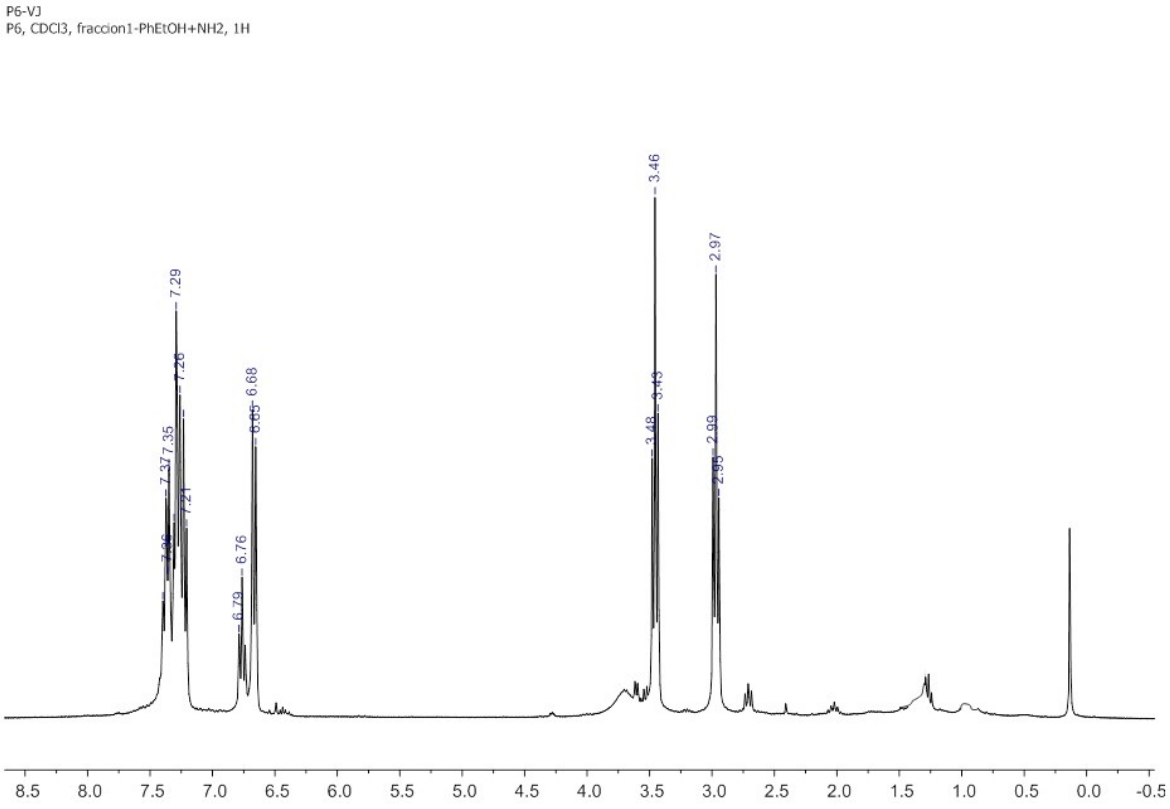

Figure S7. ^{1}H ($CDCl_3$, 298 K) NMR spectrum of *N*-phenethylaniline.

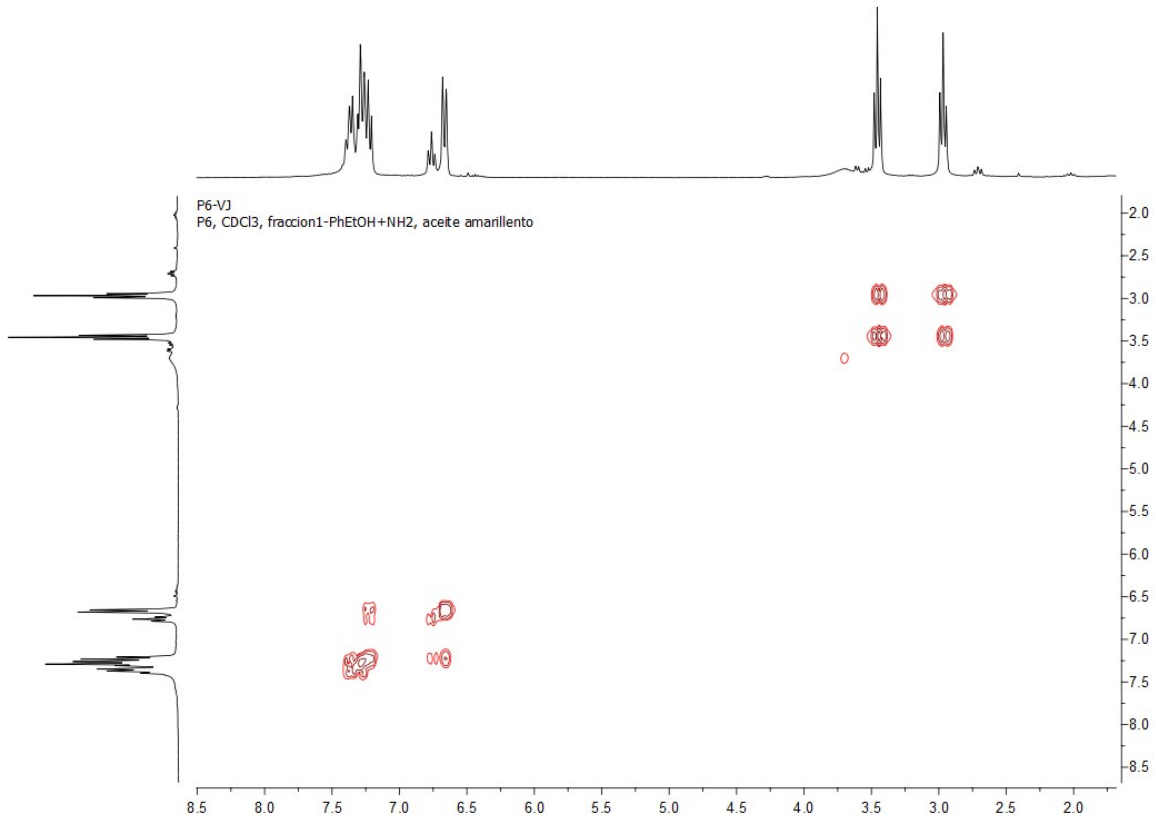

Figure S8. ^{1}H-^{1}H-cosy ($CDCl_3$, 298 K) NMR spectrum of *N*-phenethylaniline.

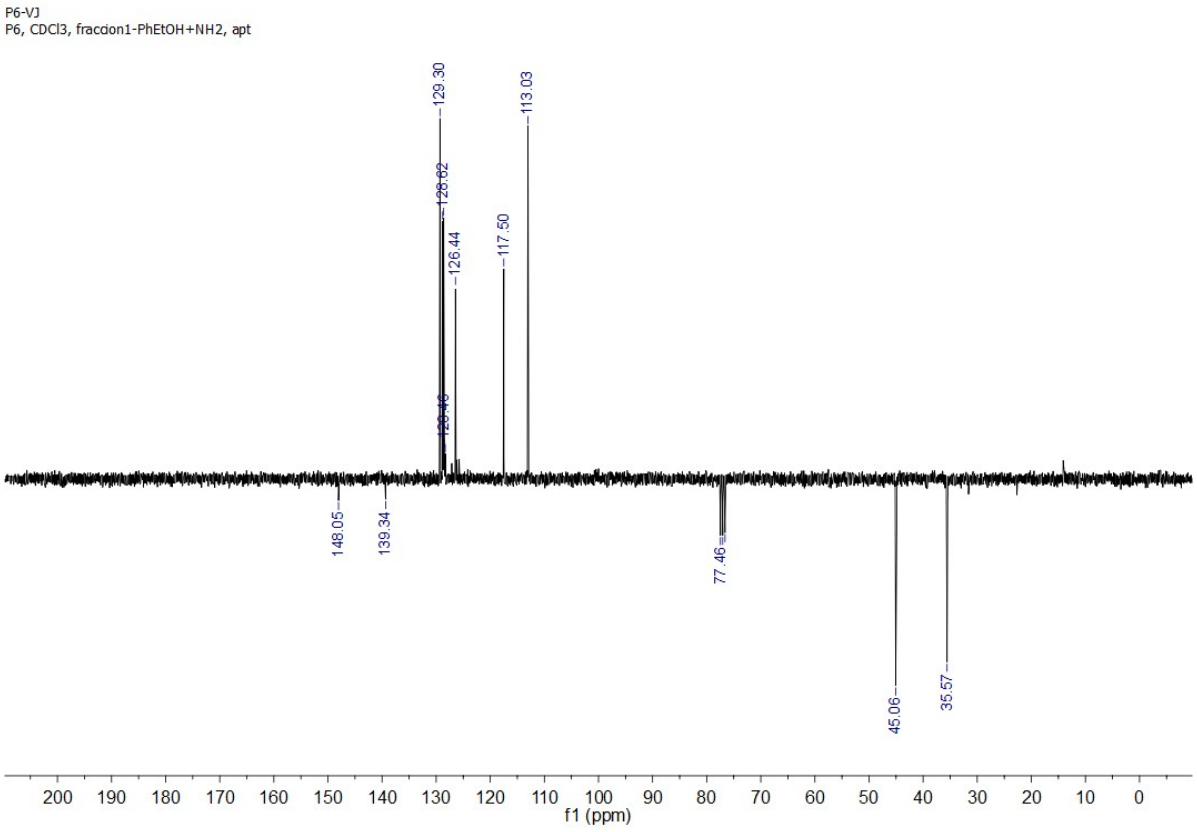

Figure S9. ^{13}C{^{1}H}-apt ($CDCl_3$, 298 K) NMR spectrum of *N*-phenethylaniline.

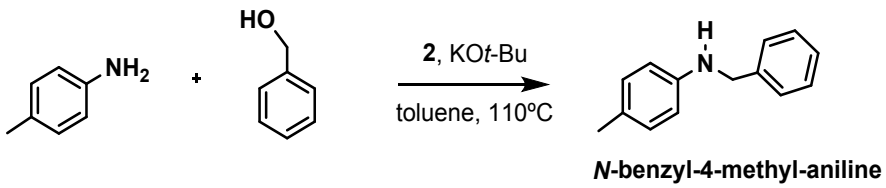

***N*-benzyl-4-methyl-aniline**

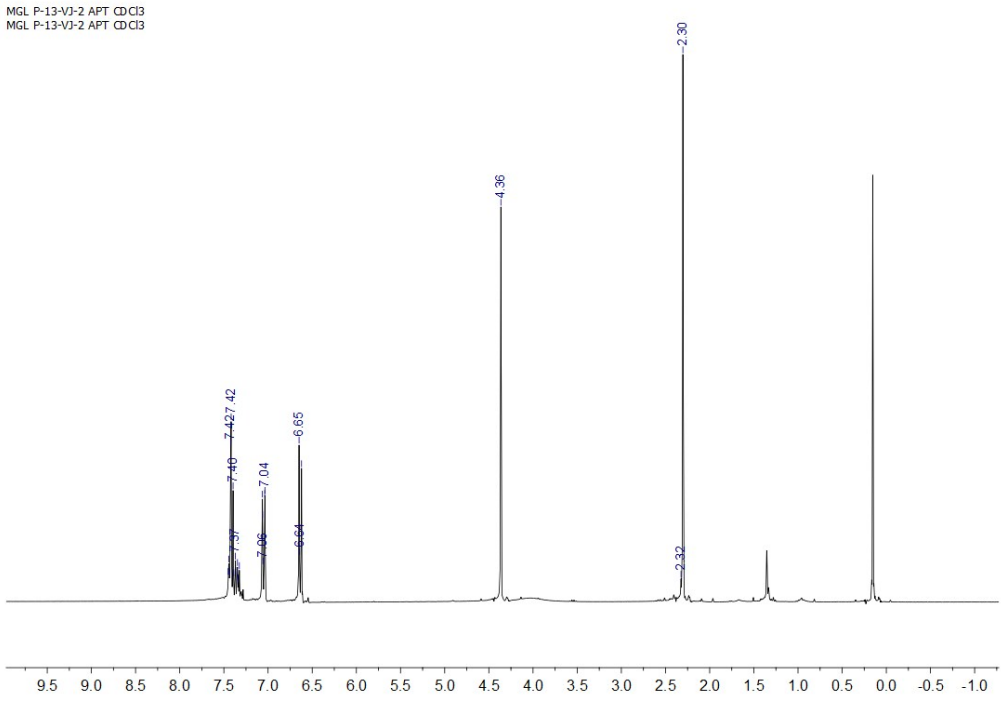

Figure S10. ^{1}H ($CDCl_3$, 298 K) NMR spectrum of *N*-benzyl-4-methyl-aniline.

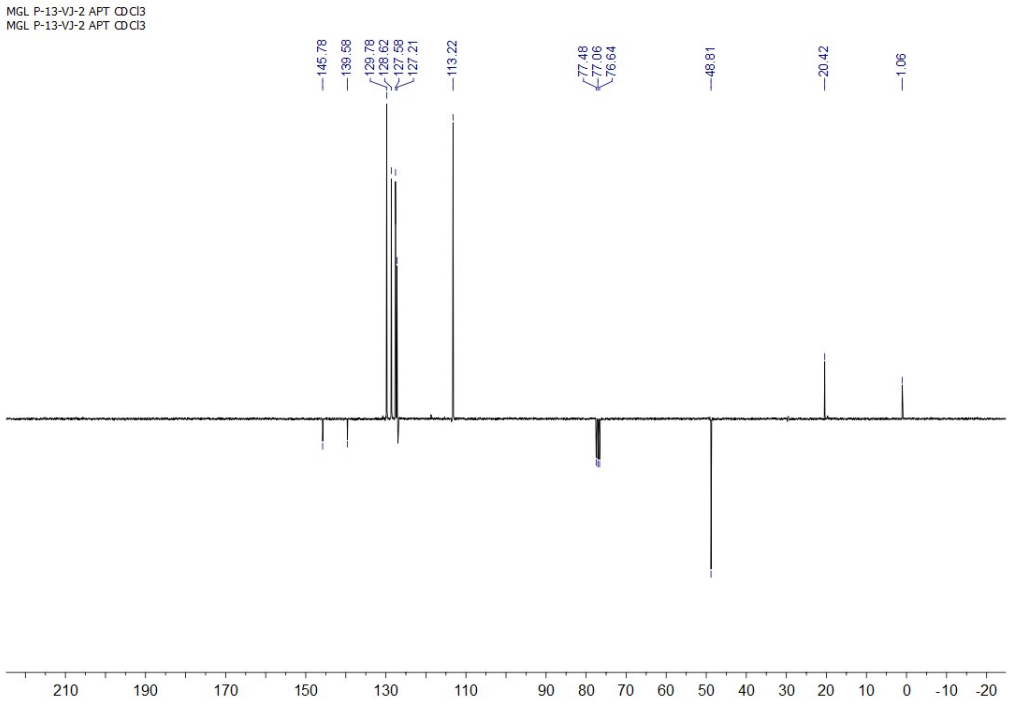

Figure S11. $^{13}C\{^{1}H\}$-apt ($CDCl_3$, 298 K) NMR spectrum of *N*-benzyl-4-methyl-aniline.

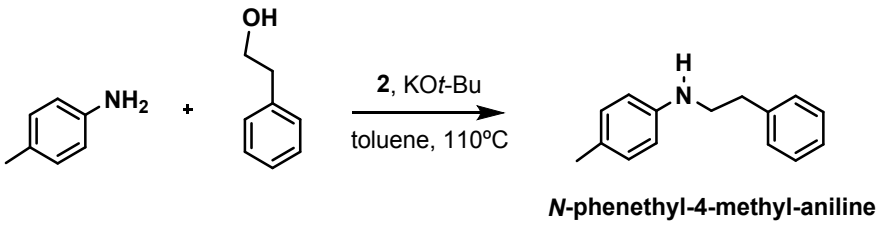

***N*-phenethyl-4-methyl-aniline**

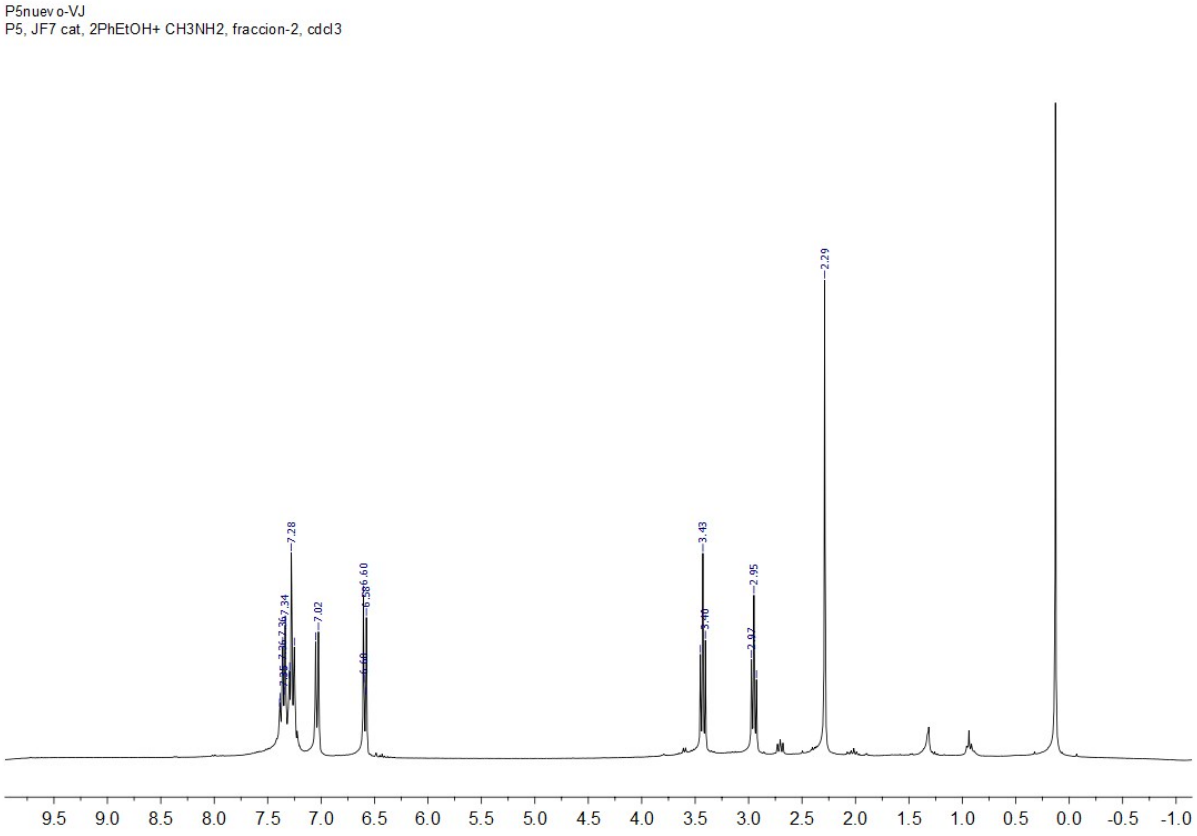

Figure S12. ^{1}H ($CDCl_3$, 298 K) NMR spectrum of *N*-phenethyl-4-methyl-aniline.

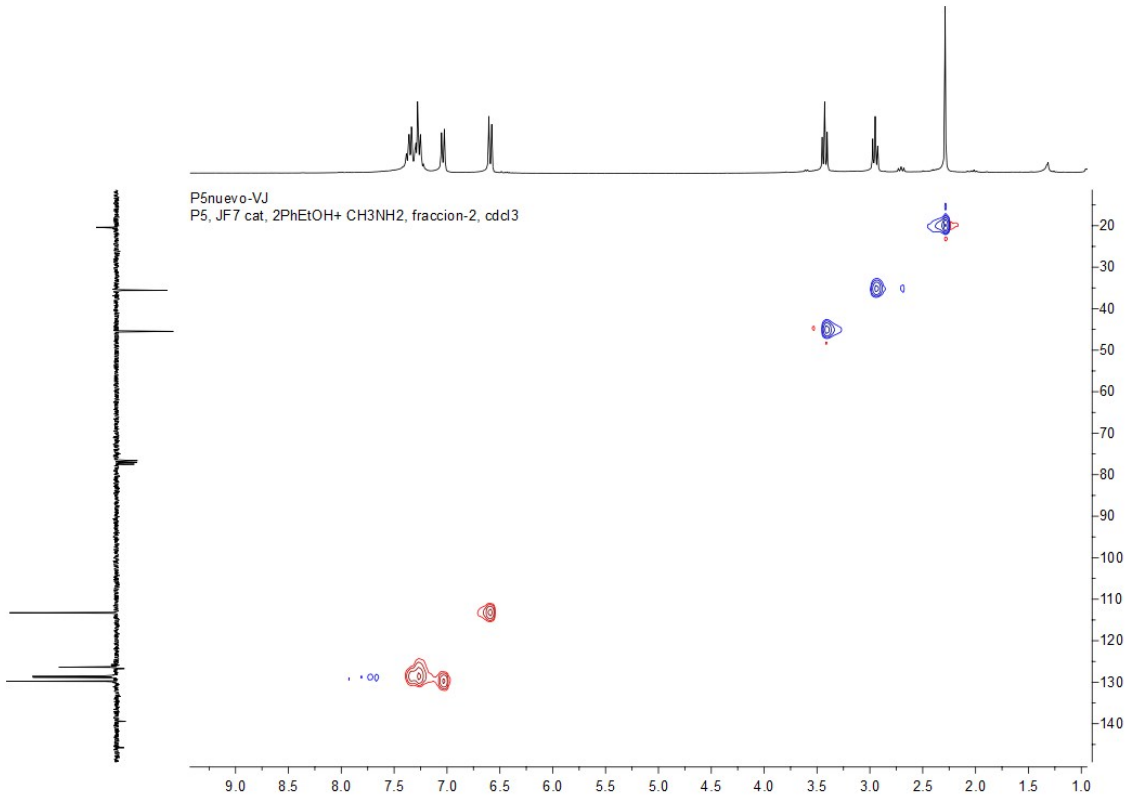

Figure S13. ^{1}H-^{13}C-apt ($CDCl_3$, 298 K) NMR spectrum of *N*-phenethyl-4-methyl-aniline.

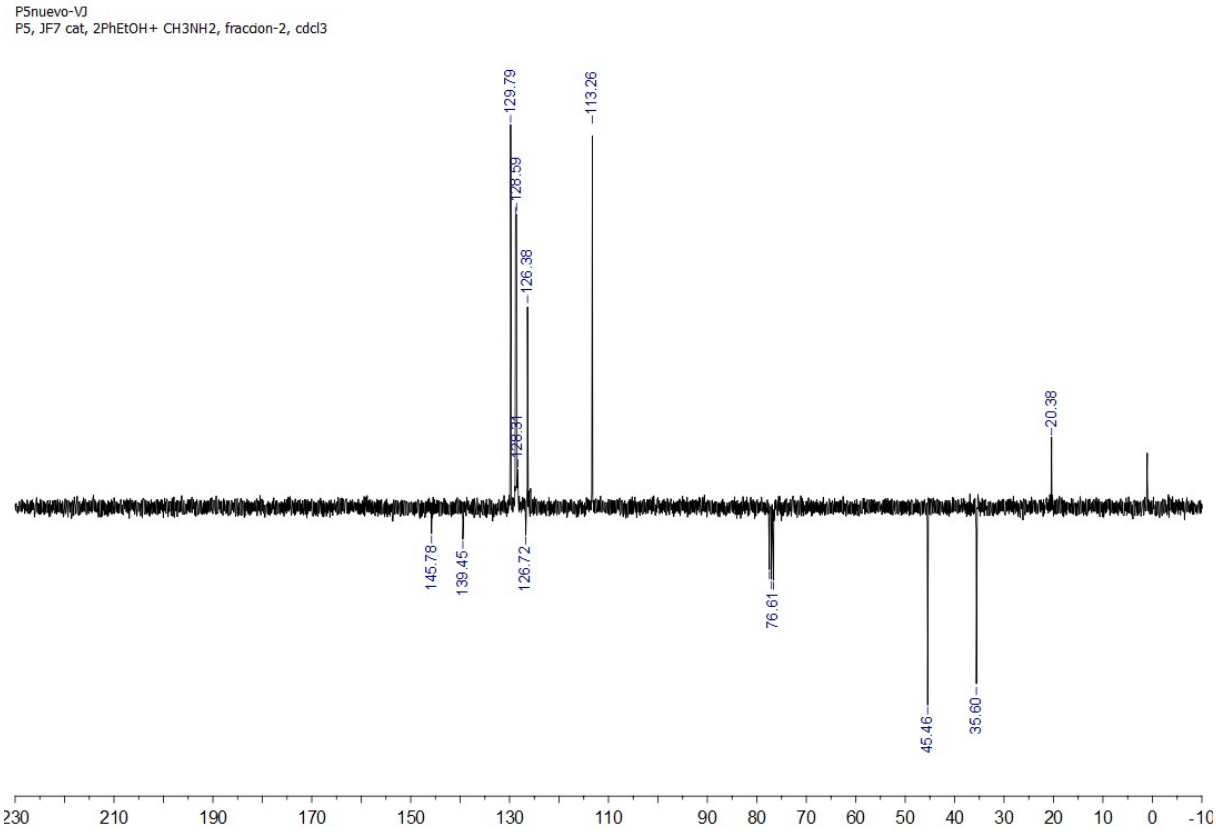

Figure S14. $^{13}C\{^{1}H\}$-apt ($CDCl_3$, 298 K) NMR spectrum of *N*-phenethyl-4-methyl-aniline.

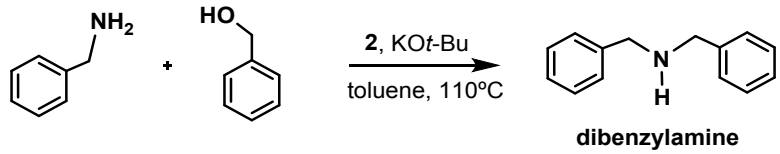

dibenzylamine

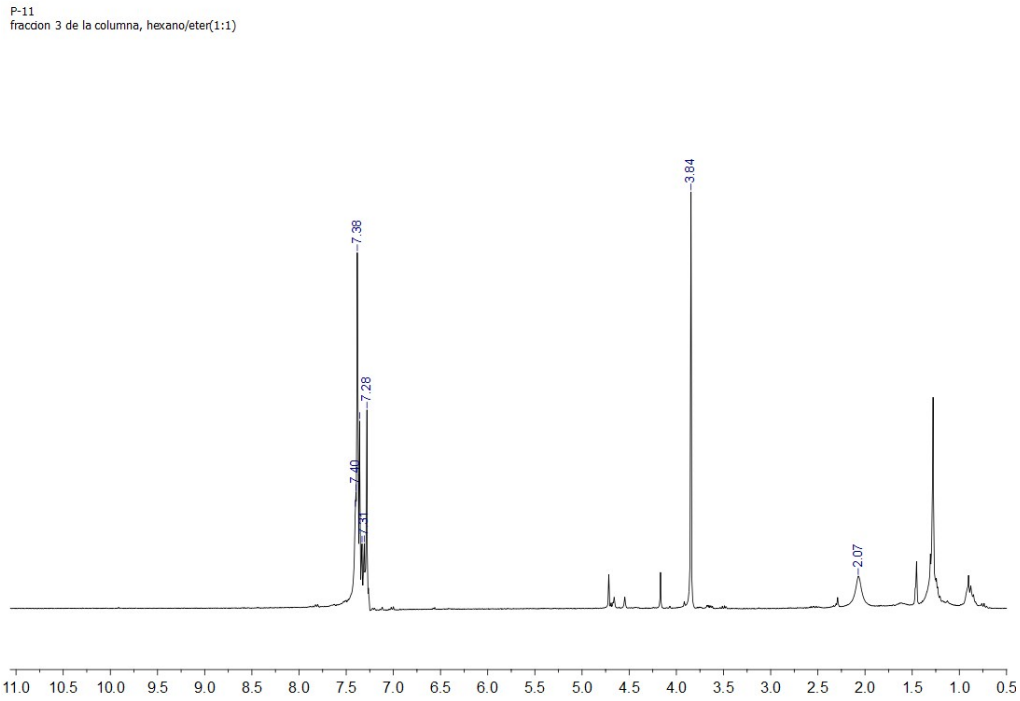

Figure S15. ^{1}H ($CDCl_3$, 298 K) NMR spectrum of dibenzylamine.

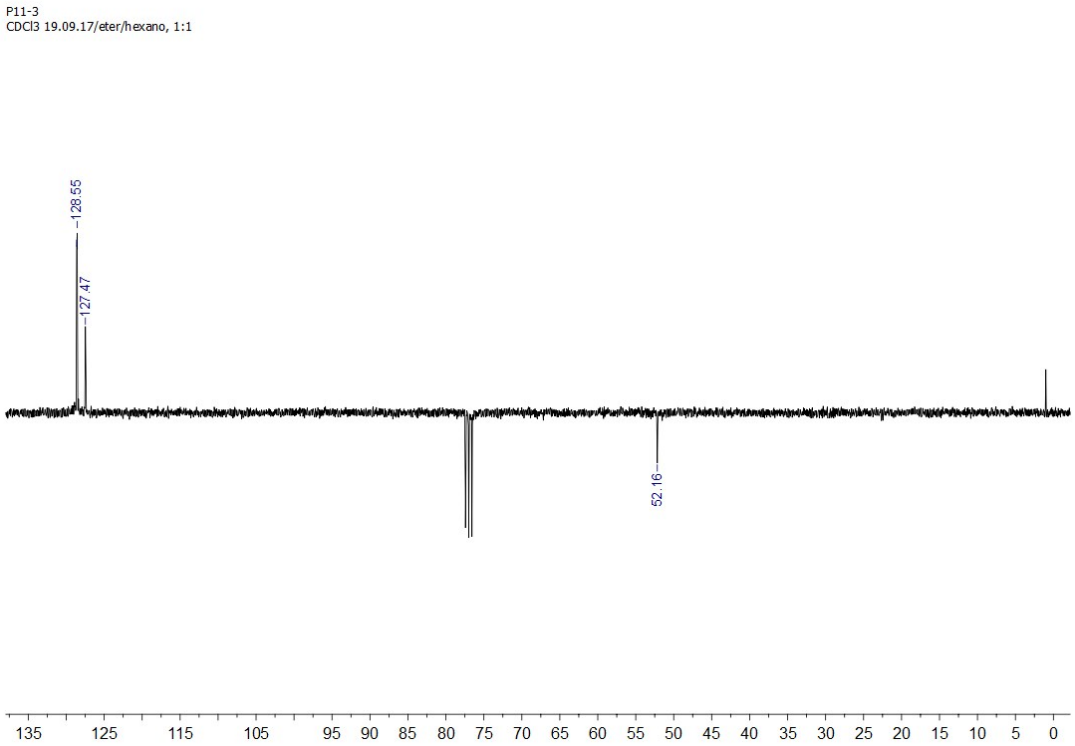

Figure S16. $^{13}C\{^{1}H\}$-apt ($CDCl_3$, 298 K) NMR spectrum of *N*-benzyl-2-phenylethan-1-amine.

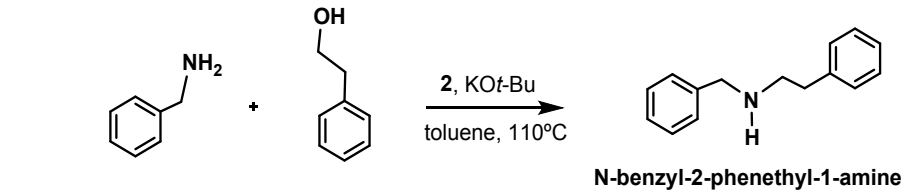

N-benzyl-2-phenethyl-1-amine

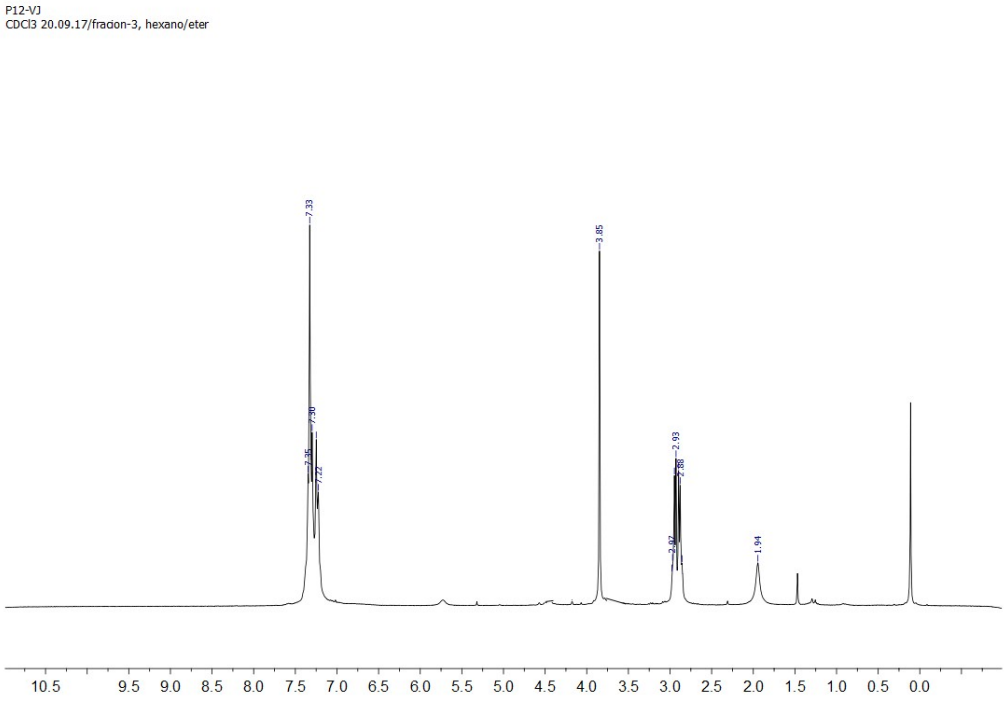

Figure S17. ^{1}H ($CDCl_3$, 298 K) NMR spectrum of *N*-benzyl-2-phenylethan-1-amine.

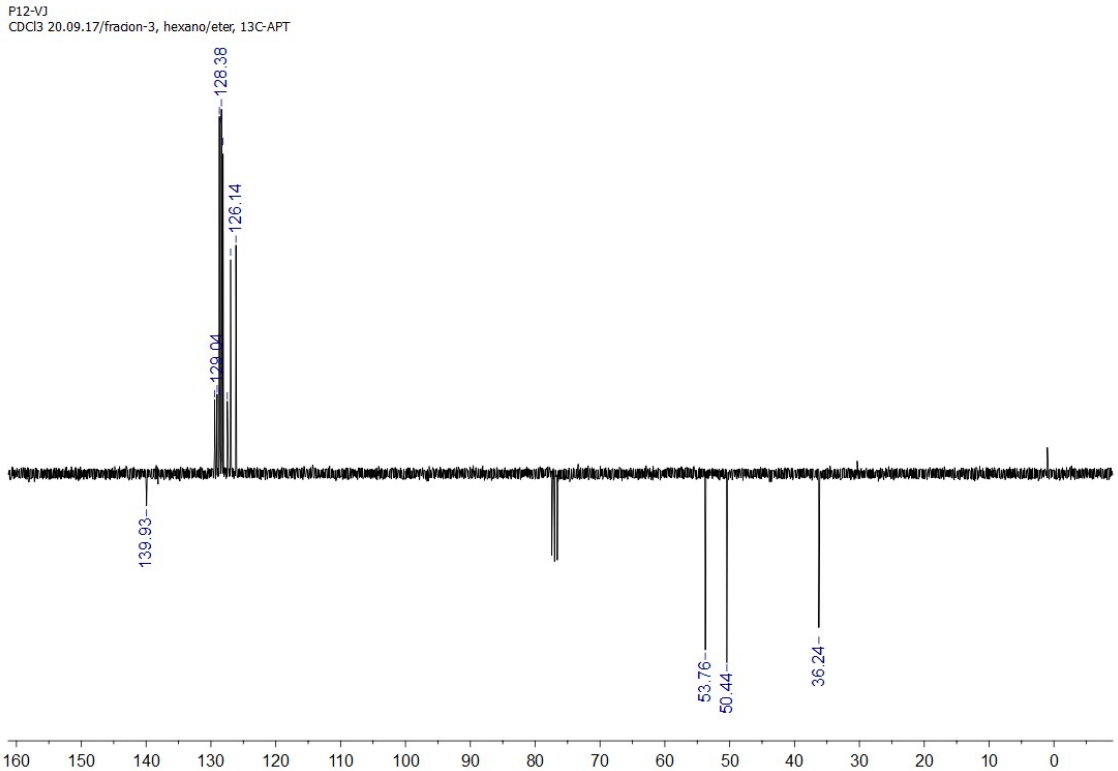

Figure S18. $^{13}C\{^{1}H\}$-apt ($CDCl_3$, 298 K) NMR spectrum of *N*-benzyl-2-phenylethan-1-amine.

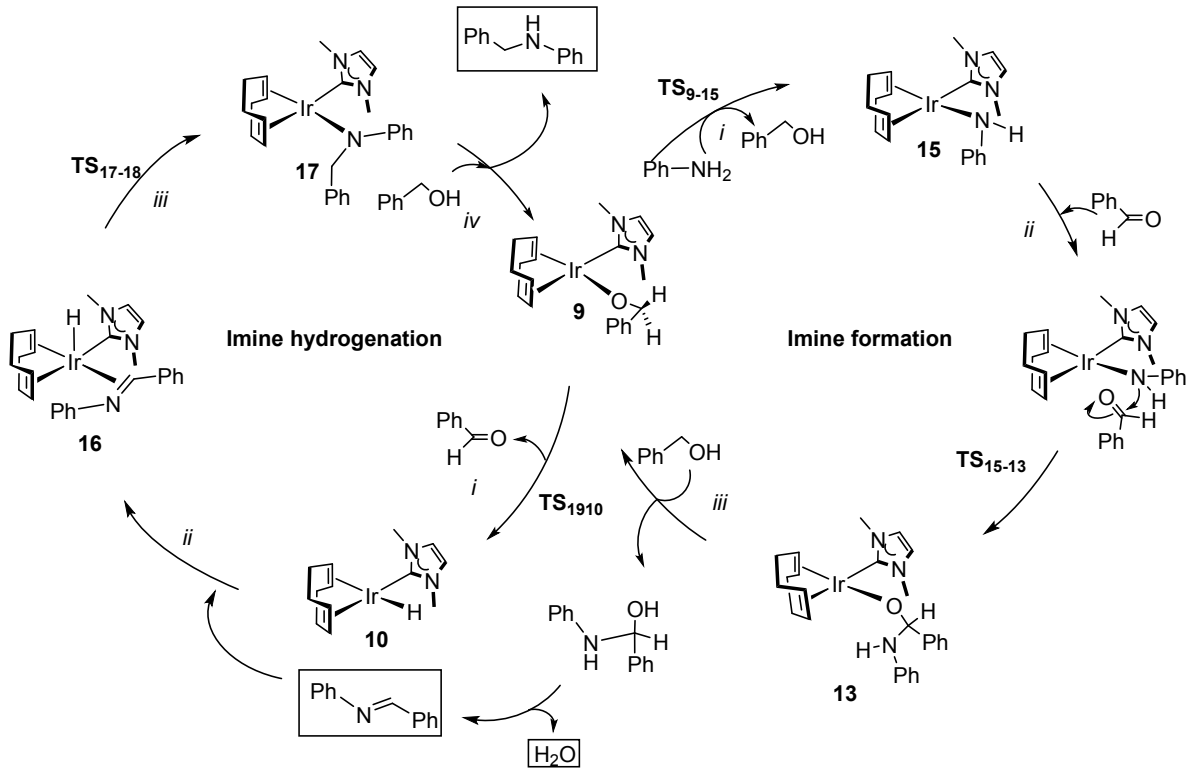

Figure S19. DFT calculated mechanism for the N-alkylation of amines with alcohols catalyzed by NHC-Ir(I) complexes.

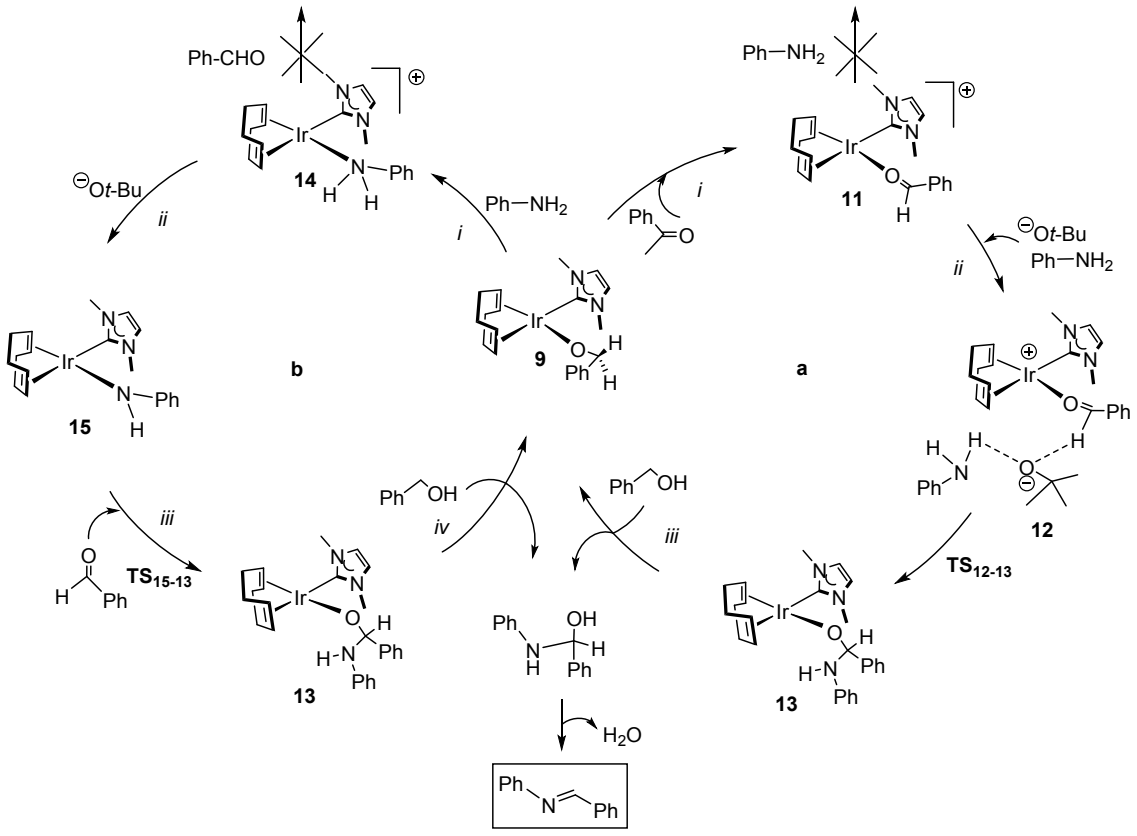

Figure S20. Alternative mechanisms for the imine formation catalyzed by NHC-Ir(I) complexes.

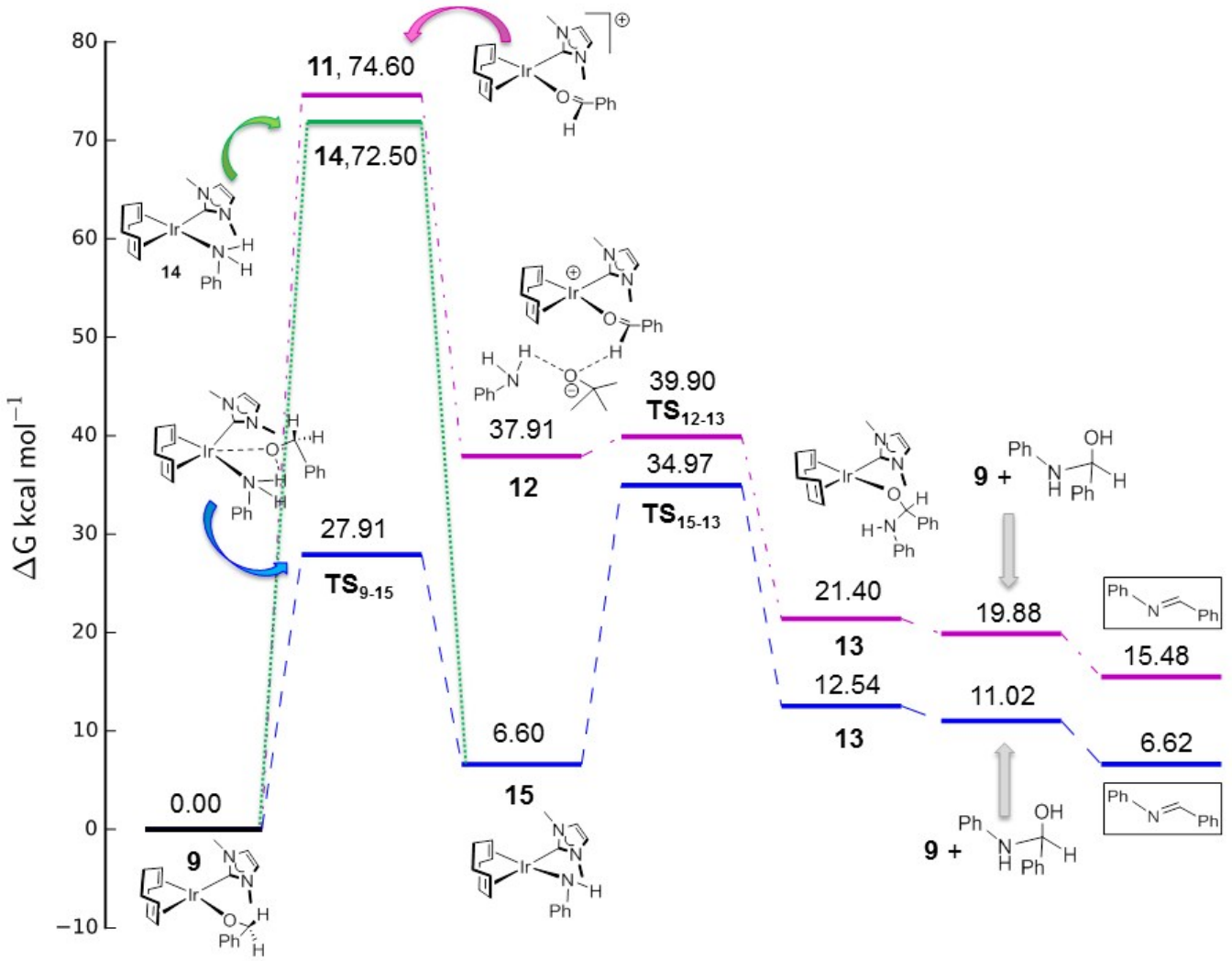

Figure S21. Energy profiles for the different pathways for the C-N bond formation step: operating mechanism (blue) and alternative mechanisms (a, pink; b, green).

Table S1. Calculated electronic and free energies.

Compound	**E(RB3PW91) (Hartree)**	**G Sum of electronic and thermal Free Energies (Hartree)**
9	-1067.5643285	-1067.184302
10	-722.09388046	-721.818141
11	-1066.8088521	-1066.436824
12	-1587.4299554	-1586.839588
13	-1353.8679317	-1353.398354
14	-1008.8770614	-1008.492860
15	-1008.4130112	-1008.043124
16	-1278.6433980	-1278.172750
17	-1278.6593847	-1278.188988
$TS_{9\text{-}10}$	-1067.5230436	-1067.143605
$TS_{9\text{-}15}$	-1355.0505187	-1354.557215
$TS_{15\text{-}13}$	-1353.83565346	-1353.362602
$TS_{16\text{-}17}$	-1278.6181018	-1278.150856
$TS_{12\text{-}13}$	-1587.4264847	-1586.835106
aniline	-287.50590162	-287.417389
benzyl alcohol	-346.649328393	-346.548078
benzoxide	-346.080620761	-345.993293
ter-butoxide	-233.017394274	-232.925931
tert-butanol	-233.602548874	-233.495488
hemiaminal	-632.955476543	-632.764551
imine	-556.546392319	-556.380921
amine prod.	-557.764948546	-557.576810
benzaldehyde	-345.444428714	-345.364698
water	-76.3946102517	-76.390699
S-9	-1413.00800630	-1412.521315
S-15	-1353.85981349	-1353.385238
S-$TS_{15\text{-}13}$-a	-1699.28170613	-1698.705060
S-$TS_{15\text{-}13}$-b	-1699.27886162	-1698.701042
S-$TS_{16\text{-}17}$	-1624.06351980	-1623.491183

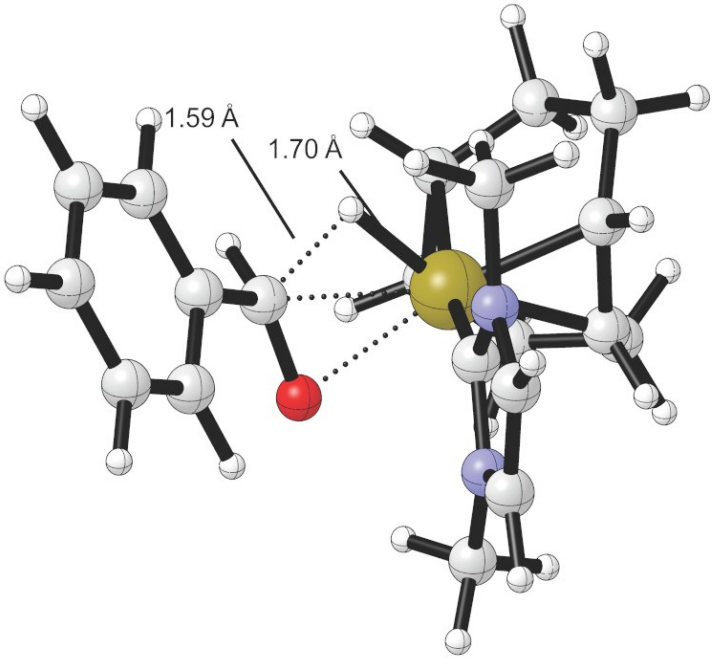

Figure S22. Transition structure $\mathbf{TS_{9\text{-}10}}$ for the formation of benzaldehyde by β-H elimination from a benzoxide ligand.

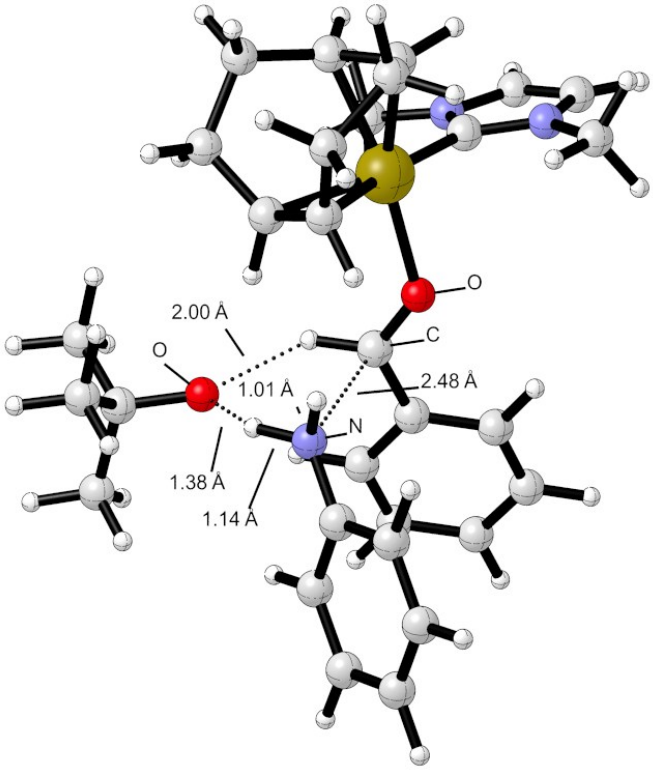

Figure S23. Transition structure $\mathbf{TS_{12\text{-}13}}$ for the nucleophilic attack of aniline on a coordinated benzaldehyde ligand.

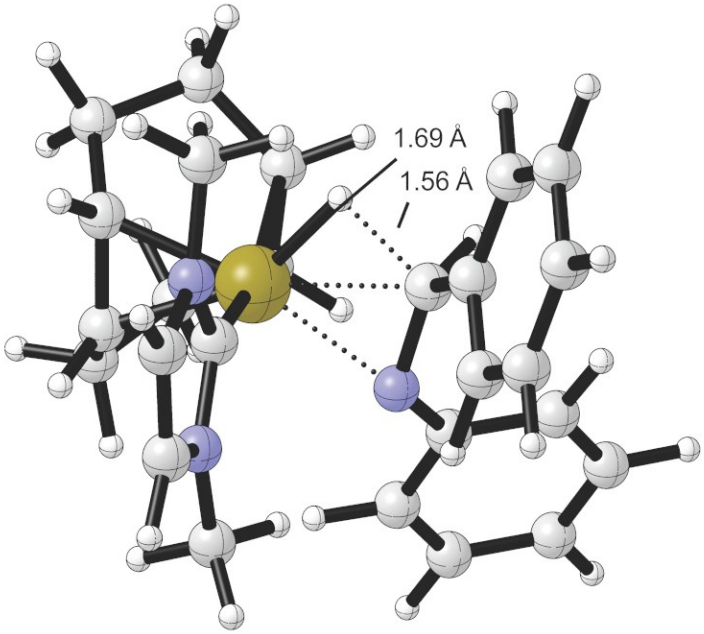

Figure S24. Transition structure $\mathbf{TS_{16\text{-}17}}$ for the insertion of imine into the Ir-H bond leading to hydrogenation.